Optical Fiber Technology 20 (2014) 158–162

Contents lists available at ScienceDirect

Optical Fiber Technology

www.elsevier.com/locate/yofte

Experimental demonstration of the maximum likelihood-based chromatic dispersion estimator for coherent receivers

Robert Borkowski [a,*], Pontus Johannisson [b], Henk Wymeersch [c], Valeria Arlunno [a], Antonio Caballero [a], Darko Zibar [a], Idelfonso Tafur Monroy [a]

[a] DTU Fotonik – Department of Photonics Engineering, Technical University of Denmark, DK-2800 Kgs. Lyngby, Denmark
[b] Photonics Laboratory, Chalmers University of Technology, SE-412 96 Gothenburg, Sweden
[c] Communication Systems Group, Chalmers University of Technology, SE-412 96 Gothenburg, Sweden

ARTICLE INFO

Article history:
Received 14 November 2013
Revised 16 January 2014
Available online 13 February 2014

Keywords:
Chromatic dispersion
Optical performance monitoring
Maximum likelihood
Digital signal processing
16 QAM
QPSK

ABSTRACT

We perform an experimental investigation of a maximum likelihood-based (ML-based) algorithm for bulk chromatic dispersion estimation for digital coherent receivers operating in uncompensated optical networks. We demonstrate the robustness of the method at low optical signal-to-noise ratio (OSNR) and against differential group delay (DGD) in an experiment involving 112 Gbit/s polarization-division multiplexed (PDM) 16-ary quadrature amplitude modulation (16 QAM) and quaternary phase-shift keying (QPSK).

1. Introduction

Linear impairments, in particular chromatic dispersion (CD) and polarization-mode dispersion (PMD) resulting from fiber transmission are now routinely mitigated by digital signal processing (DSP) in coherent receivers. This advancement allows for fiber-optic networks that no longer require dispersion compensating modules (DCMs) and two-stage amplification to perform reliable transmission. The major benefits of uncompensated links include: decrease in the noise figure (due to decrease in linear and nonlinear optical noise), reduction in link loss and latency, lower deployment capital expenditures.

As optical networks adopt flexibility and dynamic lightpath switching [1], the CD accumulated in the signal may change between two different connection requests, even if a source and destination are the same. Therefore a conventional approach, where a coherent receiver uses a static CD filter, does no longer apply. This makes an accurate adaptive CD estimation for dispersion unmanaged coherent photonic backbones indispensable.

Various approaches to non-data aided CD estimation in digital coherent receivers have been presented. One of the methods is based on parameter extraction from equalizer taps [2]. Due to a limited number of filter taps in the receiver, this solution might only be used to monitor relatively small CD, roughly corresponding to a stretch of one fiber span in long haul network. To support longer links, other methods, based on CD scanning are used. In those techniques, the space of possible CD values is searched in small steps (20–200 ps/nm [3]) and a metric value is computed for each step. A characteristic feature of this metric, often global minimum or maximum, is used to indicate successful mitigation of CD. Diverse variants of this procedure, each using a different metric, have been shown so far. A method derived from constant modulus algorithm (CMA), where the metric is based on a departure from a fixed power threshold, is used in Refs. [3,4], delay-tap sampling estimator [5,6], autocorrelation of signal power waveform [7,8], clock tone search [9–11], Gardner time error detector variance [12]. Recently, another technique have been demonstrated, where the sweep over CD values is performed automatically when applying FFT on the autocorrelation of discrete spectrum [13].

In this paper we present an experimental investigation of a method for CD estimation based on the maximum likelihood (ML) criterion [14]. The approach is experimentally verified in a transmission experiment using 112 Gbit/s polarization division multiplexed (PDM) 16-ary quadrature amplitude modulation (16 QAM) and quaternary phase-shift keying (QPSK) optical signals and its performance is compared, and found better, to an alternative (reference) method derived from constant modulus algorithm

* Corresponding author. Fax: +45 4593 6581.
E-mail address: rbor@fotonik.dtu.dk (R. Borkowski).

http://dx.doi.org/10.1016/j.yofte.2014.01.009
1068-5200

criterion from [4]. (Please notice that this is not the CMA commonly used for polarization demultiplexing.)

2. CD estimator

In this section we shortly present the maximum likelihood CD estimator. The full derivation can be found in [14].

We consider a coherent optical communication system using polarization multiplexing. The data, phase, and polarization state of the received signal are unknown, as is the differential group delay (DGD) along an unknown axis. The received signal can be expressed in the frequency domain as

$$\mathbf{R}(f) = H(f)e^{-j2\pi f\tau}\mathbf{T}(f)\mathbf{S}(f) + \mathbf{N}(f) \equiv \mathbf{X}(f) + \mathbf{N}(f),$$

where $H(f)$ is the transfer function of the CD, τ is an unknown propagation delay, the Jones matrix $\mathbf{T}(f)$ describes the polarization scrambling and DGD, $\mathbf{S}(f)$ is the Fourier transform of the transmitted signal, and $\mathbf{N}(f)$ is complex additive white Gaussian noise (AWGN) with power spectral density $N_0/2$ per each of the four real dimensions. The CD all-pass filter is described by

$$H(f) = \exp\left(-j\frac{\pi f^2\lambda^2}{c}\int_0^L D(z)\,\mathrm{d}z\right) = e^{j\pi\eta T^2 f^2},$$

where λ is the carrier wavelength, c is the speed of light, $D(z)$ is the dispersion parameter, L is the total system length, and η is the CD parameter to be estimated. The likelihood for the received signal is

$$p(\mathbb{r}|\eta,\tau,\mathbf{T},\mathbf{a}) \propto \exp\left[-\frac{1}{N_0}\int \|\mathbf{R}(f) - \mathbf{X}(f)\|^2\,\mathrm{d}f\right],$$

where we used Parseval's theorem to write the likelihood in the Fourier domain and denoted a vector representation of received signal in time domain, $\mathbf{r}(t)$, by $\mathbb{r}$. This expression depends on the data, represented by the sequence of transmitted symbols $\mathbf{a}$. To remove the dependency on $\mathbf{a}$, we use the second order Taylor expansion of $p(\mathbb{r}|\eta,\tau,\mathbf{T},\mathbf{a})$ and take the expectation with respect to $\mathbf{a}$. We thus find an approximate expression for $p(\mathbb{r}|\eta,\tau,\mathbf{T})$. Further approximations allow us to remove the dependence on τ. However, the objective function still depends on $\mathbf{T}$. We solve this by optimizing over a small number of polarization states and DGD values. We formulate the final result in terms of the received signal after matched filtering. Thus, we introduce $\mathbf{Y}(f) = P^*(f)\mathbf{R}(f)$, where $P^*(f)$ is the transfer function of the filter matched to the transmitted pulse shape. For any M-ary quadrature amplitude modulation or M-ary phase-shift keying modulation format for $M > 2$, the final estimator turns out to be

$$\hat{\eta} = \arg\max_{\eta}\max_{\mathbf{M}\in\mathcal{S}}\left|\int_{-\infty}^{\infty}\mathbf{Y}^{\mathrm{H}}(f)\mathbf{M}\mathbf{Y}(f+1/T)e^{-j2\pi\eta Tf}\,\mathrm{d}f\right|, \tag{1}$$

where the set of matrices to test is

$$\mathcal{S} = \left\{\begin{pmatrix}1 & 0\\ 0 & \pm 1\end{pmatrix}, \begin{pmatrix}0 & 1\\ \pm 1 & 0\end{pmatrix}\right\}.$$

3. Experimental setup

Fig. 1 shows the experimental setup, which can generate optical 16 QAM signal at 14 Gbaud or QPSK at 28 Gbaud. A pulse pattern generator (PPG) generates four copies of decorrelated electrical signals carrying binary pseudorandom bit sequences of length $2^{15} - 1$ (PRBS-15) which are then amplified. For 16 QAM, the PPG operates at 14 GHz and the resulting four signals are grouped in pairs, one signal from each pair is attenuated by 6 dB, and each pairs is combined in a resistive combiner. This results in two four-level signals: in-phase (I) and quadrature (Q) components for the double-nested Mach–Zehnder modulator. In the optical domain, a 16 QAM signal at 56 Gbit/s is obtained. For QPSK, two amplified PPG outputs operate at 28 Gbit/s, generating two-level I and Q signals, which results in an optical QPSK signal at 56 Gbit/s. The light source used in the transmitter is an external cavity laser (ECL) with a linewidth of 100 kHz. Polarization division multiplexing is emulated by multiplexing the signal with its delayed copy in the orthogonal polarization, creating, respectively PDM–16 QAM and PDM-QPSK optical signals at 112 Gbit/s. An erbium-doped fiber amplifier is used at the transmitter to compensate for the insertion losses.

The signal is launched into a link without dispersion compensating fiber using a commercial wavelength division multiplexing (WDM) equipment with all other WDM channels turned off. An amplified spontaneous emission (ASE) noise loading stage is used only for back-to-back performance measurements. The transmission experiment is performed over links of 240, 400, 640, and 800 km lengths by using 3, 5, 8, and 10 spans, respectively of 80 km-long standard single-mode fiber, with nominal dispersion of 16.25 ps/(nm km) at the operating wavelength. Unless stated otherwise, the input power to the first span is 0 dBm and the optical signal-to-noise ratio (OSNR) is measured at the receiver in 0.1 nm bandwidth. A variable optical attenuator before the receiver is used to keep the power ratio between the signal and the local oscillator (LO) constant. For QPSK back-to-back measurements a DGD emulator is used to introduce delays of 20, 40, 60, and 80 ps.

3.1. Digital coherent receiver

The signal is received with a phase- and polarization-diversity digital coherent receiver whose structure is outlined in Fig. 2. The receiver consists of an opto-electronic front-end and a digital signal processing (DSP) stage.

3.1.1. Opto-electronic front-end

The front-end includes two polarization beam splitters (PBS) splitting the received signal and the local oscillator into two orthogonal polarizations (H – horizontal, V – vertical), two 90° hybrids for each polarization, a set of transimpedance amplifiers (TIAs) and analog-to-digital converters (ADCs). The ADCs are provided inside a real-time digital storage oscilloscope (DSO) with a 50 GS/s with 16 GHz bandwidth. The data is sampled by the DSO and the acquired traces are processed offline.

3.1.2. Digital signal processing

The offline processing stage begins with signal resampling to two samples per symbol by spline interpolation. The downsampled signal is then fed into the CD monitor and CD equalizer block, where the signal is first divided into blocks of fixed length and transformed to frequency domain. Dispersion mitigation is then performed blockwise by a transversal frequency domain equalizer due to low, logarithmically increasing, computational complexity for increasing dispersion magnitude, as compared to time domain equalization [4]. The variable transfer function generator, $H^{-1}(CD)$, is responsible for generating an inverse of the transfer function of fiber dispersion, according to the CD value supplied by the CD monitor. The CD value is swept with a resolution of 3 ps/nm until an optimum value indicated by the metric algorithm (estimator) is found. Depending on the specific test case, either an ML-based algorithm or the reference method is implemented inside *CD monitor* block in Fig. 2. To avoid aliasing when evaluating Eq. (1), ML CD estimator shall operate with four samples per symbol. Therefore the downsampled signal is again upsampled to four samples per symbol before entering ML CD monitor. Upsampling is necessary

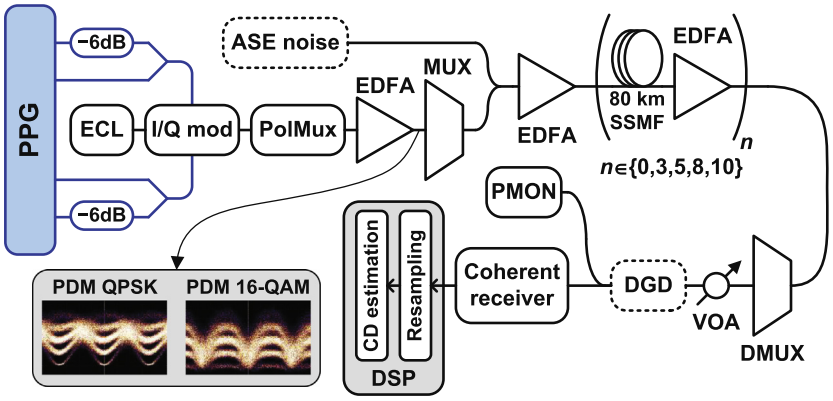

Fig. 1. The experimental setup. PPG: pulse pattern generator, ECL: external cavity laser, PolMux: polarization multiplexing stage, EDFA: erbium-doped fiber amplifier, (D) MUX: (de) multiplexer, SSMF: standard single-mode fiber, VOA: variable optical attenuator, DGD: differential group delay emulator, PMON: power monitor, DSP: digital signal processing stage.

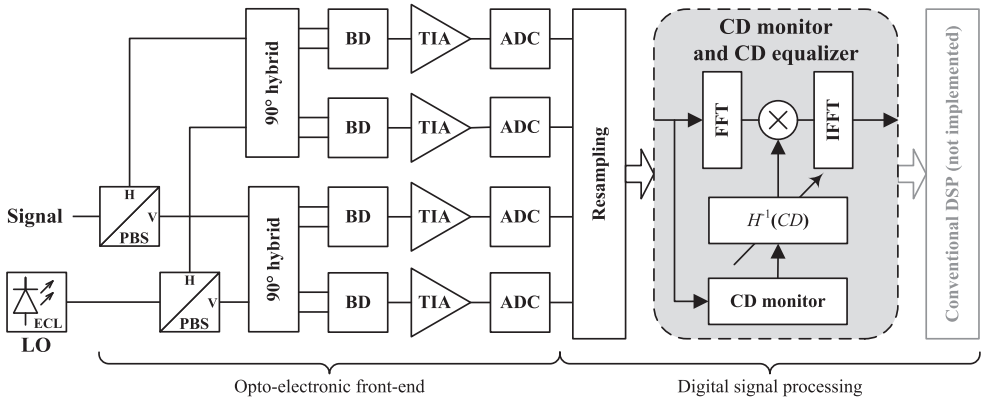

Fig. 2. Typical structure of a digital coherent receiver with CD monitoring and equalization block. The receiver in the figure monitors CD from time domain samples. LO: local oscillator, ECL: external cavity laser, PBS: polarization beam splitter, BD: balanced detector, TIA: transimpedance amplifier, ADC: analog-to-digital converter, (I) FFT: (inverse) fast Fourier transform.

to take into account the fact that the bandwidth of the transformed signal $\mathbf{Y}^{\mathrm{H}}(f)\mathbf{Y}(f+1/T)$ increases and 2 samples/symbol is not sufficient to satisfy the sampling theorem.

After the frequency domain processing, the signal is subsequently transformed to time domain. In the next step, conventional DSP algorithms for a coherent receiver (*Conventional DSP* in Fig. 2) are used. Their structure typically follow the one presented in [15]. This includes a butterfly finite impulse response filter structure which combats the residual dispersion. It is important to emphasize that the CD monitoring algorithm considered in this work do not replace any of the conventional DSP blocks of a digital coherent receiver. This is a separate and complementary block used prior to the typical coherent receiver DSP, and is aimed at mitigation of the bulk dispersion. Without this block, the subsequent DSP algorithms will fail to operate correctly as a large CD values cannot be compensated for within the blind adaptive equalizer due to convergence issues. Since we only focus on the quality of CD estimates provided by the bulk CD monitors, there was no need to include any further DSP algorithms beyond the CD equalizer and CD monitor.

4. Results and discussion

The CD estimates provided by the ML-based estimator are compared against estimates obtained with the reference method implemented with default parameters ($\xi = 1.25$, $R_a = 0.6$, $R_b = 1.5$, $R_c = 2$) [4]. The latter algorithm was chosen to provide a fair comparison base as: (i) the DSP structure in which the algorithm is implemented is very similar (the only difference is the algorithm inside *CD monitor* block in Fig. 2); (ii) previous results for that estimator report successful dispersion mitigation for both QPSK and 16 QAM modulation formats [10], which are also used in our experiment; (iii) it is well established, with an unambiguous description in the literature. The performance is measured using the standard deviation of the CD estimate, σ (in ps/nm), calculated from 1000 evaluations of sub-blocks of size N samples (Sa) within the same trace. The comparison was done with a CD scan resolution of 3 ps/nm.

Different plots of Fig. 3 show σ as a function of:

- Block size in Sa: (a) for back-to-back case (OSNR: 16 QAM 27.4 dB, QPSK 18.4 dB); (d) 240 km transmission (OSNR: 16 QAM 26.7 dB, QPSK 28.9 dB).

  In all presented cases, the standard deviation of the estimate decreases for increasing block lengths. This is explained by the fact that longer blocks allow to infer signal statistics with higher accuracy, consequently allowing for more precise dispersion estimation. The performance of ML for QPSK is shown to slightly outperform the reference. ML estimator is more accurate for 16 QAM than for QPSK, while the opposite is true for the reference method. This sets 16 QAM curves far apart, with

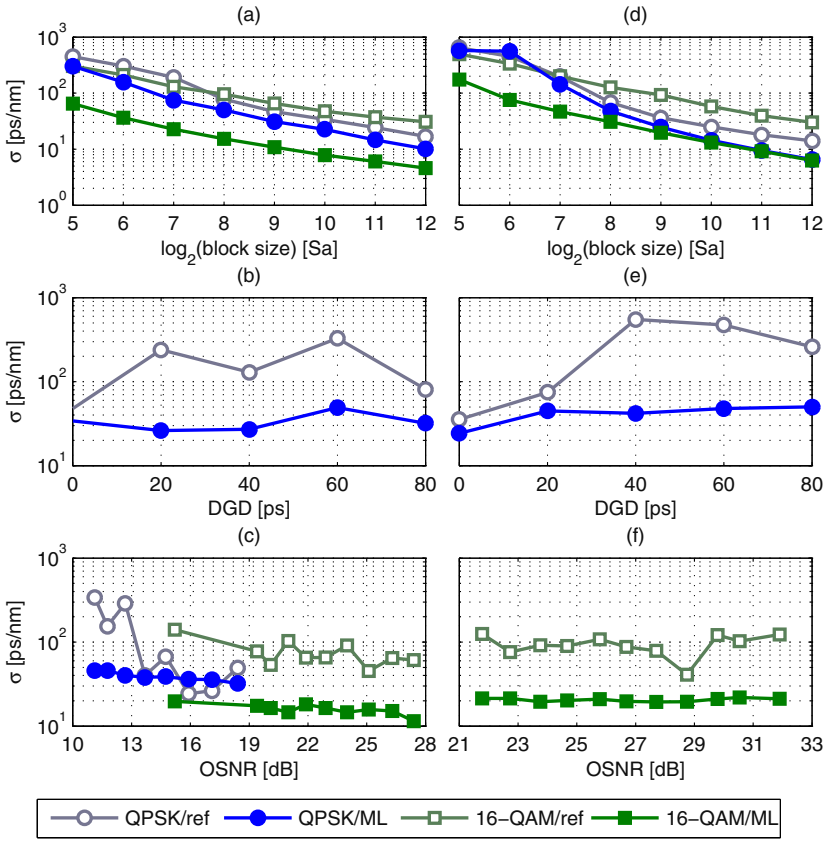

Fig. 3. Plots for back-to-back (a–c) and 240 km transmission (d–f). Plots show estimation standard deviation as a function of: (a,d) block size in samples; (b,e) DGD in ps; (c,f) OSNR in dB.

Table 1
Estimation results for all transmission distances. CD_0 – nominal CD value, m – estimated mean, Δ – mean estimation error (deviation of m from the nominal value), σ – standard deviation of the estimate.

L (km)	CD_0 (ps/nm)	OSNR (dB)	ML (ps/nm)			Reference (ps/nm)		
			m	Δ	σ	m	Δ	σ
QPSK								
0	0	18.4	−14	−14	33	−19	−19	46
240	3900	28.9	3886	−14	24	3879	−21	35
400	6500	27.0	6486	−14	36	6481	−19	287
640	10400	25.0	10397	−3	42	10396	−4	257
800	13000	22.3	13003	3	48	12994	−6	92
16 QAM								
0	0	27.4	−27	−27	11	−46	8	60
240	3900	26.7	3871	−29	20	3865	−35	90
400	6500	25.1	6471	−29	21	6470	−30	87
640	10400	23.0	10385	−15	24	10373	−27	65
800	13000	20.0	12987	−13	21	12989	−11	138

ML being significantly more accurate. The suboptimal performance of the reference estimator for 16 QAM may stem from the fact that this algorithm is derived from the constant modulus algorithm.

- DGD in ps for QPSK (constant block size of 512 Sa): (b) back-to-back (OSNR 18.4 dB); (e) 240 km transmission (OSNR 28.9 dB). Using ML estimation, standard deviation of the CD estimate is similar for all DGD values. This behaviour is expected and has been observed also in simulations [14]. The reference method, on the other hand, is sensitive to DGD and exhibits high σ for non-zero DGD.
- OSNR in dB (constant block size of 512 Sa): (c) back-to-back (by varying the amount of ASE noise); (f) 240 km transmission for 16 QAM only (the OSNR was adjusted by varying the input power to the first span from −5 dBm to 5 dBm in steps of 1 dBm).

The performance of the reference estimator deteriorates rapidly below 15 dB OSNR while ML remains almost unaffected. The improved performance of ML at low OSNR values agrees with simulation results [14]. The poor performance of the reference method in that regime is mainly caused by the outliers in CD estimates. The standard deviation of the CD estimates for

16 QAM using reference method is roughly one order of magnitude higher than for ML estimates and was also observed in subfigures (a,d). On the other hand, the ML estimator has virtually the same performance with low spread of estimates across wide range of OSNR values.

Table 1 shows CD estimation results for diverse transmission distances. It can be seen that for ML estimator the mean estimation error, Δ, which is the difference between the estimated mean and the nominal value, $\Delta = m - CD_0$, is lower in case of QPSK than for 16 QAM. On the other hand, the standard deviation of the estimate, σ is higher for QPSK. The estimates of the reference method are in general characterized by larger standard deviation than those provided by ML. In nearly all cases we notice a small underestimation, not exceeding 35 ps/nm, which might be due to the fact that the actual transmission link dispersion was lower than the assumed nominal value.

5. Conclusion

We have successfully experimentally verified the ML-based CD estimator for coherent transport networks by investigating 112 Gbit/s PDM–16 QAM and PDM–QPSK signals in the presence of variable amount of CD, ASE noise and DGD. The studied estimator was compared to an alternative method derived from the CMA criterion. The ML dispersion estimator was proven to correctly operate at OSNR below 15 dB and provided precise and repeatable CD estimates even with significant DGD. A substantial decrease of CD estimates' spread, especially for PDM–16 QAM, was observed with the ML dispersion estimator, as compared to the reference method.

Acknowledgments

We thank Neil Guerrero Gonzalez and Bangning Mao from European Research Center, Huawei Technologies Duesseldorf GmbH in Munich, Germany for their help in acquiring experimental data. We also thank Fabian Hauske for constructive comments. This work was partly supported by the EU FP7 project CHRON under Grant Agreement No. 258644.

References

[1] I. Tafur Monroy, D. Zibar, N. Guerrero Gonzalez, R. Borkowski, Cognitive heterogeneous reconfigurable optical networks (CHRON): enabling technologies and techniques, in: 2011 13th International Conference on Transparent Optical Networks, IEEE, 2011. p. Th.A1.2. doi:10.1109/ICTON.2011.5970833 <http://ieeexplore.ieee.org/lpdocs/epic03/wrapper.htm?arnumber=5970833>.

[2] F.N. Hauske, J.C. Geyer, M. Kuschnerov, K. Piyawanno, T. Duthel, C.R. Fludger, D. van den Borne, E.-D. Schmidt, B. Spinnler, H. de Waardt, B. Lankl, Optical performance monitoring from FIR filter coefficients in coherent receivers – OSA technical digest (CD), in: Optical Fiber Communication Conference/National Fiber Optic Engineers Conference, Optical Society of America, 2008. p. OThW2 <http://www.opticsinfobase.org/abstract.cfm?URI=OFC-2008-OThW2>.

[3] R. Borkowski, X. Zhang, D. Zibar, R. Younce, I. Tafur Monroy, Experimental demonstration of adaptive digital monitoring and compensation of chromatic dispersion for coherent DP-QPSK receiver, Opt. Exp. 19 (26) (2011) B728–B735, http://dx.doi.org/10.1364/OE.19.00B728. <http://www.opticsexpress.org/abstract.cfm?URI=oe-19-26-B728> and <http://www.ncbi.nlm.nih.gov/pubmed/22274095>.

[4] M. Kuschnerov, F.N. Hauske, K. Piyawanno, B. Spinnler, M.S. Alfiad, A. Napoli, B. Lankl, DSP for coherent single-carrier receivers, J. Lightw. Technol. 27 (16) (2009) 3614–3622. <http://jlt.osa.org/abstract.cfm?URI=jlt-27-16-3614>.

[5] D. Wang, C. Lu, A.P.T. Lau, S. He, Adaptive chromatic dispersion compensation for coherent communication systems using delay-tap sampling technique, IEEE Photon. Technol. Lett. 23 (14) (2011) 1016–1018, http://dx.doi.org/10.1109/LPT.2011.2151280. <http://ieeexplore.ieee.org/lpdocs/epic03/wrapper.htm?arnumber=5764498>.

[6] V. Ribeiro, S. Ranzini, J. Oliveira, V. Nascimento, E. Magalhães, E. Rosa, Accurate blind chromatic dispersion estimation in long-haul 112 Gbit/s PM-QPSK WDM coherent systems, in: Advanced Photonics Congress, OSA, Washington, DC, 2012, p. SpTh2B.3. doi:10.1364/SPPCOM.2012.SpTh2B.3 <http://www.opticsinfobase.org/abstract.cfm?URI=SPPCom-2012-SpTh2B.3>.

[7] Q. Sui, A.P.T. Lau, C. Lu, Fast and robust blind chromatic dispersion estimation using auto-correlation of signal power waveform for digital coherent systems, J. Lightw. Technol. 31 (2) (2013) 306–312. <http://jlt.osa.org/abstract.cfm?URI=jlt-31-2-306>.

[8] F.C. Pereira, V.N. Rozental, M. Camera, G. Bruno, D.A.A. Mello, Experimental analysis of the power auto-correlation-based chromatic dispersion estimation method, IEEE Photon. J. 5 (4) (2013) 7901608, http://dx.doi.org/10.1109/JPHOT.2013.2272782. <http://ieeexplore.ieee.org/lpdocs/epic03/wrapper.htm?arnumber=6557429>.

[9] F.N. Hauske, Z. Zhang, C. Li, C. Xie, Q. Xiong, Precise, Robust and least complexity CD estimation, in: Optical Fiber Communication Conference/National Fiber Optic Engineers Conference 2011, OSA, Washington, DC, 2011, p. JWA032. doi:10.1364/NFOEC.2011.JWA032 <http://www.opticsinfobase.org/abstract.cfm?URI=NFOEC-2011-JWA032>.

[10] R.A. Soriano, F.N. Hauske, N. Guerrero Gonzalez, Z. Zhang, Y. Ye, I. Tafur Monroy, Chromatic dispersion estimation in digital coherent receivers, J. Lightw. Technol. 29 (11) (2011) 1627–1637. <http://jlt.osa.org/abstract.cfm?URI=jlt-29-11-1627>.

[11] C. Malouin, P. Thomas, B. Zhang, J. O'Neil, T. Schmidt, Natural expression of the best-match search godard clock-tone algorithm for blind chromatic dispersion estimation in digital coherent receivers, in: Advanced Photonics Congress, OSA, Washington, DC, 2012, p. SpTh2B.4. doi:10.1364/SPPCOM.2012.SpTh2B.4. <http://www.opticsinfobase.org/abstract.cfm?URI=SPPCom-2012-SpTh2B.4>.

[12] J.C. Diniz, S. Ranzini, V. Ribeiro, E. Magalhães, E. Rosa, V. Parahyba, L.V. Franz, E.E. Ferreira, J. Oliveira, Hardware-efficient chromatic dispersion estimator based on parallel gardner timing error detector, in: Optical Fiber Communication Conference/National Fiber Optic Engineers Conference 2013, OSA, Washington, DC, 2013, p. OTh3C.6. doi:10.1364/OFC.2013.OTh3C.6. <http://www.opticsinfobase.org/abstract.cfm?URI=OFC-2013-OTh3C.6>.

[13] C. Malouin, M. Arabaci, P. Thomas, B. Zhang, T. Schmidt, R. Marcoccia, Efficient, Non-data-aided chromatic dispersion estimation via generalized, FFT-based sweep, in: Optical Fiber Communication Conference/National Fiber Optic Engineers Conference 2013, OSA, Washington, DC, 2013, p. JW2A.45. doi:10.1364/NFOEC.2013.JW2A.45. <http://www.opticsinfobase.org/abstract.cfm?URI=OFC-2013-JW2A.45>.

[14] H. Wymeersch, P. Johannisson, Maximum-likelihood-based blind dispersion estimation for coherent optical communication, J. Lightw. Technol. 30 (18) (2012) 2976–2982. <http://jlt.osa.org/abstract.cfm?URI=jlt-30-18-2976>.

[15] S.J. Savory, Digital coherent optical receivers: algorithms and subsystems, IEEE J. Sel. Topics Quant. Electron. 16 (5) (2010) 1164–1179, http://dx.doi.org/10.1109/JSTQE.2010.2044751. <http://ieeexplore.ieee.org/lpdocs/epic03/wrapper.htm?arnumber=5464309>.